Blind Source Separation for Wireless Networks: A Tool for Topology Sensing (Invited Paper)

Enrico Testi(✉), Elia Favarelli, and Andrea Giorgetti

Alma Mater Studiorum – University of Bologna, Via dell'Università 50, Cesena, Italy
{enrico.testi4,elia.favarelli2,andrea.giorgetti}@unibo.it

Abstract. In this work, a tool for topology sensing of a non-collaborative wireless network using power profiles captured by radio-frequency (RF) sensors is proposed. Assuming that the features of the network (i.e., the number of nodes, medium access control (MAC) and routing protocols) are unknown and that the sensors observe signal mixtures because of the wireless medium, blind source separation (BSS) is used to separate the traffic profiles. Successively, the topology of the network is inferred by detecting causal relationships between the separated streams. According to the numerical results, the proposed tool senses the topology with promising accuracy when operating in mild shadowing conditions, even with a relatively low number of radio-frequency (RF) sensors.

Keywords: Blind source separation · Topology sensing · Wireless networks · Cognitive radio

1 Introduction

Thanks to the impressive advances in research in communication technologies, networks' importance is strongly growing within our society. A network of sensors deployed to collect environmental data, a community of social network users, or a tactical network suited for the exchange of data between soldiers are only a small part of the vastness of common networks.

In this scenario, to predict the traffic flow, to estimate the network connectivity, detect communities, infer the communications between nodes, help optimization and orchestration are only a few examples of tasks that can benefit the topology sensing. Focusing on wireless networks, while cognitive radios (CRs) are currently exploiting spectrum sensing, a detailed knowledge on how a network uses the radio-frequency (RF) medium can be obtained by the structure of the network, and it might help the development of more performing spectrum sharing algorithms [1,4,20,22].

In many of the scenarios mentioned above, it seems mandatory that the topology of the network is inferred from external, without being a part of it

G. Caso et al. (Eds.): CrownCom 2020, LNICST 374, pp. 29–42, 2021.
https://doi.org/10.1007/978-3-030-73423-7_3

or increasing the network overhead. For this reason, the possibility of reconstructing the topology of a network from observed signals at some nodes with almost zero prior knowledge is being investigated nowadays [10,28,33]. Assuming that the main features of the network, such as the number of nodes, their accurate position, and the traffic types are unknown, our objective is to infer its topology by observing it from external. Firstly, an estimate of the number of transmitting nodes (sources) is provided, then the transmitted power profiles as if they were measured at the sensors are separated using blind source separation (BSS). Finally, we compare well-known topology inference tools based on Granger causality (GC) and transfer entropy (TE) accounting for noise and propagation impairments.

1.1 Existing Works

In literature, numerous methodologies for network topology inference have been proposed and tested. Some of them require the packet's content to be accessible, which might not always be granted, and increment the total network overhead [10,28]. Others require access to information at endpoints, falling into the network tomography category [31,33].

The topology sensing problem can be tackled using statistical tests built on temporal models that relate different time series, as theorized by Pearl [16] and Granger [5]. In particular, the auto-regressive (AR) models based test proposed by Granger in [5], became the reference for numerous causal analysis and inference methodologies proposed in the last decades. As an alternative, a technique to infer causal relationships within networks based on a variant of the classic GC, named asymmetric Granger causality (AGC), is exploited in [11]. A worth-mentioning technique to model causal relationships is represented by the Hawkes point processes [30]. Another state-of-the-art methodology for causality detection is TE, which exploits the amount of directed transfer of information between two time series [18]. In [19], a TE-based topology sensing method is proposed and compared to the GC test. The presented topology inference methods require the temporal characterization of the signals transmitted by each node of the network. For this reason, the packet streams have to be reconstructed as if they were measured at the nodes. Due to the fact that the RF sensors acquire a mixture of the signals generated by the nodes because of the wireless medium, an unmixing operation to extract the transmitted power profiles is necessary [9,32].

Various methods for unmixing signals, e.g., matrix factorization [3] and tensor decomposition [2,8], have been proposed in literature. In this work, we combine the principal component analysis (PCA) and Fast-independent component analysis (ICA) methodologies [6]. We then propose a specific solution to associate the reconstructed sequences and compare some of the topology inference algorithms mentioned above. In Sect. 5, we inspect how shadowing impacts the reconstruction of the packet profiles, and, consequently, the reliability of the sensed topology [23,24].

1.2 Application Scenarios

The designed tool senses the topology of a wireless network, assuming that it is non-collaborative. This could be necessary, i.e., because it is private, encrypted, and not accessible, or it is a contender in the use of shared spectrum. This is the reason why the BSS and the topology sensing have to be carried out from the outside. To motivate this assumption, two generic examples of application are briefly described in the following:

- Spectrum optimization and reuse: let us consider a wireless network aiming to detect if another network is competing for the use of the same portion of the radio spectrum (also not legally). The nodes repeatedly sense the RF spectrum [7,12] to collect power samples and forward them to the fusion center (FC). It is in charge of the detection of the competing wireless network, performing BSS and topology inference. Once the adversarial topology is sensed, the wireless network is capable of optimizing its communications with respect to the structure and the spectrum usage of the competing network. Of course, the time necessary to probe the radio spectrum worsens the throughput of the network while optimizing the dynamic spectrum allocation.
- Tactical network: in this scenario, a network of RF sensors is deployed within an adversarial network's area to obtain information about it. The sensors acquire the radio spectrum samples and forward them to the designed FC. It performs BSS and topology inference. If the specifications of the sensor network (i.e., the energy consumption) allow it, the topology can be inferred in real-time.

Throughout the paper, capital boldface letters denote matrices, lowercase bold letters denote vectors, $(\cdot)^{\mathrm{T}}$ is the transpose operator, $\odot$ is the element-wise product, $|\cdot|$ is the modulus operator, and $||\cdot||_p$ is the l_p-norm. With $\mathbf{v}_{h,:}$ and $\mathbf{v}_{:,g}$ we represent the hth row, and the gth column of the matrix $\mathbf{V}$ respectively, and with $\mathbf{v}_{h,g:k}$ we select the elements between the gth and the kth entry of the hth row of $\mathbf{V}$. $\mathcal{N}(\mu, \sigma^2)$ represents a real normal distribution with mean μ and variance σ^2, $\mathbb{E}\{\cdot\}$ returns the expected value, and $\langle\cdot\rangle$ returns the sample mean.

The rest of this work is structured as follows. The system model is introduced in Sect. 2. In Sect. 3, the blind source separation problem and the proposed solutions are described in detail. In Sect. 4, two of the state-of-the-art techniques for topology inference mentioned in Sect. 1.1 are presented. Numerical results are shown in Sect. 5 and conclusions are deduced in Sect. 6.

2 System Model and Problem Formulation

Let us consider a network of M RF sensors and an adversarial (non-collaborative) wireless network of N nodes deployed within a square area of side L_{a}.[1] Let us assume that the network's technical specifications (i.e., number of nodes, routing

[1] The BSS requires a coarse estimate of the network nodes position, therefore it can be performed by the sensor network before the tasks summarized in Fig. 1 [14,15].

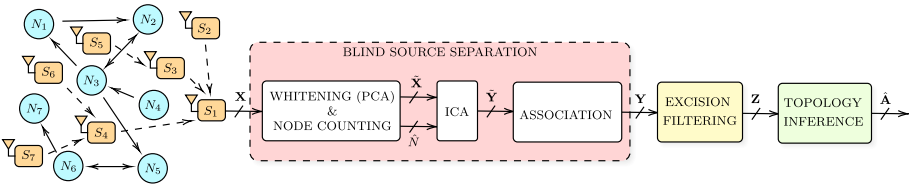

Fig. 1. Block scheme of the proposed tool: sensor network, BSS and topology inference.

protocols) are unknown. Usually, the network's topology can be seen as a directed graph and represented as its associated adjacency matrix $\mathbf{A} \in \{0,1\}^{N\times N}$ where

$$a_{h,k} = \begin{cases} 1 & \text{if the data flow from node } h \text{ to } k \\ 0 & \text{otherwise.} \end{cases}$$

The objective is to estimate the adjacency matrix, $\widehat{\mathbf{A}}$, of the wireless network from the power profiles captured by the RF sensors within an observation window of duration T_{ob}. The sensors cannot interact with the observed network. Therefore, to perform the data processing summarized in Fig. 1, the demodulation of the received signals is not required, so that a simple energy detector (ED) is needed at the receiver [12,26].

2.1 Data Acquisition and Channel Model

The streams of packets transmitted by each node of the network are time series arranged as rows of the matrix $\mathbf{P} \in \mathbb{R}^{N\times K}$ where K is the number of power samples collected. The channel is represented by the mixing matrix $\mathbf{H} \in \mathbb{R}^{M\times N}$, whose entries are the channel gains $h_{m,n}$ between sensor m and node n.

The effect of shadowing between the nodes and the sensors is modeled by a log-normal distributed random matrix $\mathbf{S}$ whose elements are

$$s_{m,n} = \exp(\sigma_{\text{S}} G_{m,n}) \quad m = 1,\ldots,M, \;\; n = 1,\ldots,N$$

where $G_{m,n}$ are independent, identically distributed (i.i.d.) zero mean Gaussian random variables (r.v.s) with unit variance and shadowing parameter σ_{S}.[2] Moreover, assuming conventional energy detection, the thermal noise at the output of the integrator can be modeled as a constant ν added to each received sample.[3]

[2] Usually, the shadowing parameter is expressed as the standard deviation of the received power in deciBel, i.e., $\sigma_{\text{S}}(\text{dB}) = \frac{10}{\ln 10}\sigma_{\text{S}}$.

[3] The noise term in the ED is a central chi-squared r.v. with a number of degrees of freedom, N_{DOF}, proportional to the time-bandwidth product. When N_{DOF} is large, the noise term can be considered constant. As detailed in Sect. 5 we consider a system with bandwidth $W = 20\,\text{MHz}$ (i.e., WiFi channel) and an integration time $T_{\text{i}} = 10\,\mu\text{s}$, hence $N_{\text{DOF}} = 2WT_{\text{i}} = 400$.

Therefore, the matrix of the received power profile $\mathbf{X} \in \mathbb{R}^{M \times K}$ can be written as

$$\mathbf{X} = (\mathbf{S} \odot \mathbf{H})\mathbf{P} + \nu \mathbf{1}_{M,K} \tag{1}$$

where $\mathbf{1}_{M,K}$ is an $M \times K$ matrix of all ones. Note that the matrix $\mathbf{P}$ of the transmitted traffic profiles of the wireless network is somehow implicitly contained in $\mathbf{X}$. Nevertheless, the extraction of the desired packet streams is challenging because of physical layer impairments (i.e., propagation and noise), packet collisions, and multiple access interference.

3 Blind Source Separation

BSS is a statistical tool which purpose is to unmix the source signals (i.e., $\mathbf{P}$) from the mixture of observations (i.e., $\mathbf{X}$), when the mixing matrix (i.e., $\mathbf{H}$) is unknown [32]. Here we assume that the problem is overdetermined, that is $M \geq N$ (more sensors than sources).

3.1 Whitening and Estimation of the Number of Sources

For signal unmixing to be effective, data have to be manipulated so that there are N whitened mixtures [32]. Since we assumed that the number of nodes N is unknown, it has to be estimated.

Firstly, the row-wise mean is subtracted from $\mathbf{X}$, centering the mixtures. Then, a linear transformation named PCA is applied to the signals to whiten their components. Given the sample covariance matrix of the observations $\mathbf{\Sigma} = \frac{1}{K}\mathbf{X}\mathbf{X}^{\mathrm{T}}$, the eigenvalue decomposition $\mathbf{\Sigma} = \mathbf{U}\mathbf{\Lambda}\mathbf{U}^{\mathrm{T}}$ is performed. $\mathbf{U}$ is the eigenvectors matrix, and $\mathbf{\Lambda}$ is the diagonal matrix of the eigenvalues, Λ_i, with $i = 1, \ldots, M$, sorted in descending order. Then, the whitening matrix can be written as $\mathbf{Q} = \mathbf{\Lambda}^{-\frac{1}{2}}\mathbf{U}^{\mathrm{T}}$. The number of sources $\hat{N}$ is estimated using the minimum description length (MDL) criteria proposed in [13,27], such that

$$\hat{N} = \underset{n \in \{1,..,M\}}{\arg\min} \{\mathsf{MDL}(n)\} \tag{2}$$

where n is the unknown model order. Once $\hat{N}$ is estimated, the mixture is projected onto a new subspace which dimensionality is reduced from M to $\hat{N}$. This is accomplished by a projection matrix $\tilde{\mathbf{Q}}$ obtained from the first $\hat{N}$ rows of $\mathbf{Q}$, so that the whitened mixture can be written as $\tilde{\mathbf{X}} = \tilde{\mathbf{Q}}\mathbf{X}$.

3.2 Independent Component Analysis

ICA is a well-known method which goal is to find a linear representation of non-gaussian data so that the components are statistically independent. Here we apply ICA to unmix the transmitted packet streams (implicitly contained in $\mathbf{P}$). ICA allows us to estimate the unmixing matrix $\mathbf{W} \in \mathbb{R}^{\hat{N} \times \hat{N}}$ such that

$$\tilde{\mathbf{Y}} = \mathbf{W}^{\mathrm{T}}\tilde{\mathbf{X}} \tag{3}$$

Algorithm 1: Unmixed signals association

In : Separated components $\tilde{\mathbf{Y}}$, $\hat{N}$, $\mathbf{D}$
Out: Aligned reconstructed power profiles $\mathbf{Y}$

for n *from* 1 *to* $\hat{N}$ **do**
  $h \leftarrow \arg\min_m \{d_{m,n}\}$
  for k *from* 1 *to length of* $\tilde{\mathbf{y}}_{:,1}$ **do**
    $peaks_k \leftarrow \max\{\text{corr}(\tilde{\mathbf{y}}_{k,:}; \mathbf{x}_{h,:})\}$ †
  end
  $p \leftarrow \arg\max_k \{\mathbf{peaks}\}$
  $\mathbf{Y}_{n,:} \leftarrow \tilde{\mathbf{y}}_{p,:}$
  $\tilde{\mathbf{Y}} \leftarrow \tilde{\mathbf{Y}}/\tilde{\mathbf{y}}_{p,:}$ ‡
end

† $\text{corr}(\mathbf{c}; \mathbf{d})$ returns the cross-correlation between $\mathbf{c}$ and $\mathbf{d}$. ‡ $\tilde{\mathbf{Y}}/\tilde{\mathbf{y}}_{p,:}$ removes the pth row from $\tilde{\mathbf{Y}}$.

where $\tilde{\mathbf{Y}} \in \mathbb{R}^{\hat{N} \times K}$ is the matrix of the separated signals. Due to the particularity of the application here we propose the well-known Fast-ICA iterative algorithm, with kurtosis as a non-linear function, and decorrelation based on the Gram-Schmidt scheme [6].

Unfortunately, ICA presents an ambiguity in the order of the recovered signals; thus $\mathbf{P}$ could be obtained from $\tilde{\mathbf{Y}}$ permuting its rows. An ad-hoc solution to this problem is proposed in the next section.

3.3 Unmixed Signals Association

We propose an iterative method to match the reconstructed signals to the nodes of the wireless network. For convenience, the matrix $\mathbf{D} \in \mathbb{R}^{M \times \hat{N}}$, whose entries $d_{m,n}$ are the two-dimensional distances between sensor m and node n, is defined. The proposed algorithm is the following:

- Firstly, a node n is selected from the nodes of the wireless network and its nearest sensor m is found.
- Then, the signal acquired by sensor m is correlated with all the reconstructed signals (rows of $\tilde{\mathbf{Y}}$) separately.
- The row $\tilde{\mathbf{y}}_{p,:}$ showing the highest positive correlation peak matches with node n and is copied into the nth row of $\mathbf{Y}$, accordingly.
- Finally, the matched node is removed from the list of all the possible nodes, the pth sequence is deleted from $\tilde{\mathbf{Y}}$ and the algorithm is iterated from the beginning.

The algorithm is further detailed in Algorithm 1. Its complexity results $\mathcal{O}(\hat{N} \log \hat{N})$, making it also applicable to networks with a large number of nodes.

3.4 Excision Filter

The output $\mathbf{Y}$ of the signal association has residual crosstalk due to the presence of noise and shadowing, and it has to be removed, e.g., by an excision filter.

The signals in $\mathbf{Y}$ have been processed to obtain sequences of 0s and 1s arranged in a matrix $\mathbf{Z}$. In particular, the element $z_{n,k}$ contains 1 if node n is sending a packet at the time sample k and 0 otherwise. To do so, we use the received samples to detect the event "packet sent" by the conventional binary hypothesis test. The threshold λ_n is set as a fraction $q \in [0, 1]$ of the maximum of $\mathbf{y}_{n,:}$, i.e.,

$$\lambda_n = q \cdot \max_k \{y_{n,k}\}, \quad n = 1, \ldots, N. \tag{4}$$

4 Topology Inference Algorithms

In this section, the topology sensing methodologies, namely GC and TE, adopted in this work are briefly presented.

4.1 Granger Causality

GC method relies on linear L-order AR models. Considering two rows of $\mathbf{Z}$ corresponding to the time series of the transmitted power streams of nodes i and j, respectively, $\mathbf{z}_i$ and $\mathbf{z}_j$, two AR models can be identified

$$\mathcal{H}_1 : z_{j,k} = \sum_{l=1}^{L} \beta_l z_{j,k-l} + \sum_{l=1}^{L} \gamma_l z_{i,k-l} + \varepsilon_k \tag{5}$$

$$\mathcal{H}_0 : z_{j,k} = \sum_{l=1}^{L} \delta_l z_{j,k-l} + \omega_k \tag{6}$$

where $\{\beta_l\}_{l=1}^{L}$, $\{\gamma_l\}_{l=1}^{L}$, and $\{\delta_l\}_{l=1}^{L}$ are the regression coefficients, and ε_k, ω_k, are samples of independent additive white Gaussian noise (AWGN). The model (5) is formulated according to hypothesis $\mathcal{H}_1$, considering the possibility of a causal relationship between the two traffic streams. At the same time, the model (6) is the null hypothesis $\mathcal{H}_0$, assuming that the entries of $\mathbf{z}_i$ do not contribute in the inference of $\mathbf{z}_j$. If $\mathbf{z}_i$ does not cause $\mathbf{z}_j$ the prediction errors of the two models are approximately equal. On the other hand, if $\mathbf{z}_i$ *Granger causes* $\mathbf{z}_j$ the error of model (5) is less than the one of (6). In [17,25] a GC test based on squared sum of residuals is proposed

$$\mathsf{GC}_{i \to j} = \frac{\sum_{t=1}^{T} |\omega_t|^2 - \sum_{t=1}^{T} |\varepsilon_t|^2}{\sum_{t=1}^{T} |\varepsilon_t|^2} \cdot \frac{T - 2K - 1}{K} \underset{\mathcal{H}_0}{\overset{\mathcal{H}_1}{\gtrless}} \theta \tag{7}$$

where $T = K - L$ and K is the length of the time series. Since both the model errors, ε_k and ω_k, follow a normal distribution, the sum of squared residuals is distributed as a central chi-squared. For this reason, the test (7) results in the ratio of chi-squared r.v.'s, giving a $\mathcal{F}$-distribution [25]

$$\mathsf{GC}_{i \to j} \sim \mathcal{F}(L, T - 2L - 1).$$

A fixed false alarm probability, detailed in Sect. 5, determines the threshold θ.

4.2 Transfer Entropy

A criterion to quantify the information flow between two random processes exploiting a variant of conditional mutual information named TE is proposed in [18]. Considering two rows of $\mathbf{Z}$ corresponding to the time series of the transmitted power streams of nodes i and j, respectively, modeled as random processes, the TE from i to j can be expressed as

$$\mathsf{TE}_{i\to j}(R,Q) = \mathcal{I}(z_{j,k}; \mathbf{z}_i^-, \mathbf{z}_j^-) = \mathbb{E}\left\{ \log_2 \frac{p(z_{j,k}|\mathbf{z}_i^-, \mathbf{z}_j^-)}{p(z_{j,k}|\mathbf{z}_j^-)} \right\} \tag{8}$$

where $\mathbf{z}_i^-$ and $\mathbf{z}_j^-$ denote the samples of $\mathbf{z}_i$ and $\mathbf{z}_j$ preceding the time instant k, respectively. Usually, conditional probability densities require the knowledge of infinite past samples of the time series to be evaluated. Anyway, in this formulation, TE is calculated considering only a finite number of past samples for $\mathbf{z}_i$ and $\mathbf{z}_j$ [18]. Thus, the considered time lags for the two time series are given by R and Q, respectively. To obtain the decision threshold θ, the null distribution of the TE has to be approximated using the collected samples [19], choosing a predefined false-alarm probability. Then, the test is

$$\mathsf{TE}_{i\to j} \underset{\mathcal{H}_0}{\overset{\mathcal{H}_1}{\gtrless}} \theta. \tag{9}$$

The response generated by the dataflow from node i to node j might present a delay, i.e., when sending an acknowledgment (ACK). Hence, an interaction delay parameter, n_0, to introduce an offset in the starting point from which the time lag is calculated, is proposed in [29]. The comprehensive definition of TE can be finally written as

$$\mathsf{TE}_{i\to j}(R,Q,n_0) = \mathcal{I}(z_{j,k}; \mathbf{z}_{i,k-n_0-1:k-n_0-R}, \mathbf{z}_{j,k-1:k-Q}). \tag{10}$$

The interaction delay is taken into account only for the time series $\mathbf{z}_i$.

If for a wireless node i, we calculate $\mathrm{TE}_{i\to j}(R,Q,n_0)$, $j = 1,\ldots,N$ with $j \neq i$, and then apply the test described above for each pair $\{i,j\}$, we identify a set of likely neighbours of node i. To lower the number of false neighbors, they can be tested one more time with a slightly different version of TE named conditional transfer entropy (CTE). In this way, the effects of all the detected neighbors on the causal inference are considered. CTE from node i to j is defined as

$$\mathsf{CTE}_{i\to j}(R,Q,n_0,g) = \mathcal{I}(z_{j,k}; \mathbf{z}_{i,k-n_0-1:k-n_0-R}|\mathbf{z}_{j,k-1:k-Q}, \mathbf{z}_{g,k-1:k-Q}) \tag{11}$$

where $g = 1,\ldots,N$ with $g \neq i,j$. For further details about the CTE algorithm please refer to [19].

5 Numerical Results

In this section, the effect of channel impairments on the performance of BSS is evaluated, and the topology sensing methodologies described in Sect. 4 are

compared. As a case study, we simulated an IEEE 802.11*s* ad-hoc network, with channel width of 20 MHz and center frequency $f_0 = 2.412$ GHz, on the *ns3* network simulator. As mentioned above, the wireless network is located in a square area of side $L_\mathrm{a} = 10$ m. The transmit power of the nodes of the wireless network is $P_\mathrm{T} = 10$ dBm, while the thermal noise power at the receivers is $\sigma_\mathrm{N}^2 = -93$ dBm. The path-loss follows a power-law, with channel gain $h'_{m,n} = h_0(\frac{d_0}{d_{m,n}})^\nu$ where the loss exponent is $\nu = 3$, the reference distance is $d_0 = 1$ m, and $h_0 = -60.1$ dB. The bandwidth of the RF sensor is $W = 20$ MHz, while the integration time is $T_\mathrm{b} = 10\,\mu$s, hence $N_\mathrm{DOF} = 2WT_\mathrm{b} = 400$. The size of data packets is fixed to 1024 Byte, while the ACKs have a size of 112 Byte. The offered traffic of each node is 1 Mb/s.

The excision filter parameter, λ_n, is set as in (4) with $q = 0.7$. The time lags of the topology inference algorithms are set as $L = 4$, $R = 2$, $Q = 1$, and $n_0 = 3$ according to the Akaike information criterion (AIC) [21]. The false alarm probability for the decision threshold is set to 10^{-2} for both the algorithms. The results presented in this section are obtained from the simulations of $M_\mathrm{top} = 100$ different mesh topologies. For each of the simulated topologies, $M_\mathrm{mc} = 100$ Monte Carlo trials are performed to randomly deploy the nodes and sensors within the landscape. Usually, the topology of a network is represented by a sparse adjacency matrix $\mathbf{A}$. Thus, the accuracy, a standard non-weighted metric, is not a suitable figure of merit for the evaluation of the topology sensing performance. For this reason, in this work the detection probability (or recall), $p_\mathrm{D}^{h,k}$, and the false alarm probability (or false positive rate), $p_\mathrm{FA}^{h,k}$, of the directed link from node h to node k, defined as

$$p_\mathrm{D}^{h,k} = \mathbb{P}\{\hat{a}_{h,k} = 1 | a_{h,k} = 1\}$$
$$p_\mathrm{FA}^{h,k} = \mathbb{P}\{\hat{a}_{h,k} = 1 | a_{h,k} = 0\},$$

have been adopted. In the following, we refer to p_D and p_FA as the detection and false alarm probabilities, respectively, averaged over all the possible network connections.

Table 1. List of the parameters adopted during the simulations.

Parameter Set	A_1	A_2	B_1	B_2	C_1	C_2
ρ_S (nodes/m^2)	0.3	0.3	0.2	0.2	0.1	0.1
σ_S (dB)	3	6	3	6	3	6

The sensed topologies represent the topology of the network in a snapshot taken during the observation time, $T_\mathrm{ob} = 1$ s.

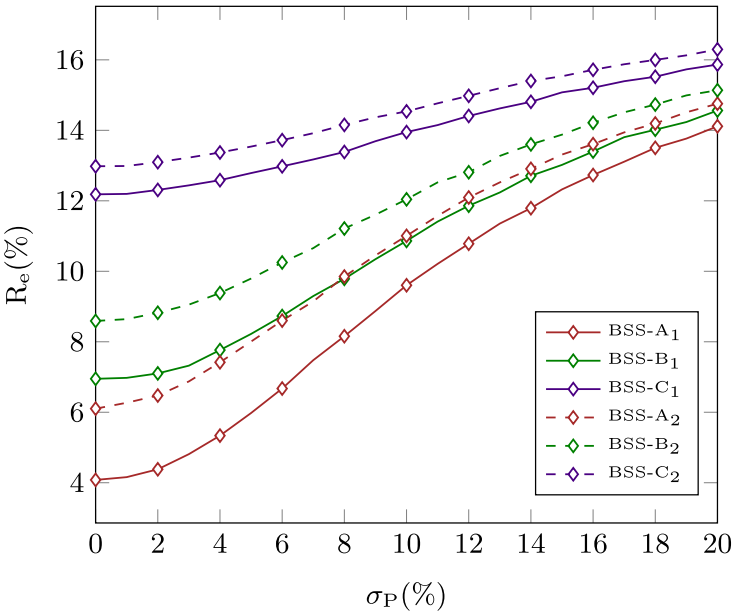

Fig. 2. BSS algorithm performance as a function of the standard deviation σ_P of the uncertainty on the position of the wireless nodes, the shadowing parameter σ_S and the density ρ_S.

5.1 BSS Reconstruction Error

As a figure of merit to quantify the effectiveness of BSS we adopted the reconstruction error, defined as

$$R_e = \frac{\#\text{ of wrong samples}}{\#\text{ of total samples}} = \frac{||\mathbf{Z} - \bar{\mathbf{P}}||_1}{N \cdot K}$$

where the matrix $\bar{\mathbf{P}}$ has entries $\bar{p}_{n,k} = 1$ if node n is transmitting in the kth bin, i.e., $p_{n,k} > 0$, and 0 otherwise. Due to the fact that the signals association can be degraded by a non-perfect knowledge of the position of the nodes, we introduce uncertainty by adding a normal distributed r.v. with standard deviation σ_P to the real coordinates. The impact of the number of sensors on the signal separation methods' performance is characterized by the density of sensors ρ_S, defined as the number of sensors per square meter. Table 1 summarizes all the configurations of parameters adopted during the simulations.

The BSS performance tests are shown in Fig. 2. In particular, the proposed method has been tested varying the standard deviation $\sigma_P(\%)$, defined as percentage of the dimension of the scenario, the shadowing parameter σ_S, and the density ρ_S. The figure shows how the reconstruction error rises when increasing σ_P, even at high densities of sensors, i.e., $\rho_S = 0.3$. Moreover, the curves is shifted upward when the shadowing intensity is increased, reaching an error $R_e = 16\%$ with $\sigma_S = 6\,\text{dB}$ and $\sigma_P = 20\%$.

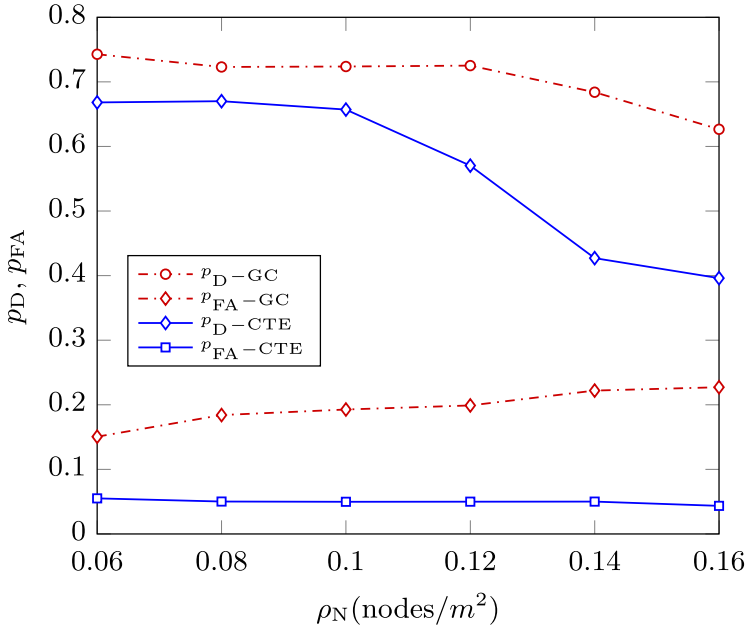

Fig. 3. p_D and p_{FA} of the topology sensing techniques varying the density of nodes ρ_N for $\rho_S = 0.3$ sensors/m^2 and $\sigma_S = 3$ dB.

5.2 Topology Inference and Number of Nodes

To provide a strong comparison between the topology sensing methodologies presented in Sect. 4, the density of wireless nodes per square meter, ρ_N, is varied across the simulations. The BSS that precedes the topology inference was performed with $\rho_S = 0.3$ sensors/m^2, $\sigma_S = 3$ dB and $\sigma_P = 0$. Note that an increase in the number of nodes within the network area rises the collision probability, which inevitably translates into a stronger network congestion. The CTE method presents the lower p_{FA}, but the p_D is lower than the GC. This means that the error on the unmixing of the signals impacts more CTE than GC (Fig. 3).

5.3 Impact of Shadowing

In a realistic scenario, the quality of the time series reconstructed after the BSS might be degraded by the presence of shadowing. Such impairment impacts the performance of the algorithms. On this point, it is important to study the accuracy of the algorithms with different propagation characteristics. In Fig. 4, it is shown how an increase in σ_S drops the performance of the algorithms. Here we set the density of sensors $\rho_S = 0.3$ sensors/m^2, the density of nodes $\rho_N = 0.06$ nodes/m^2, and $\sigma_P = 0$. Again, CTE presents a false alarm rate lower than the GC method, but p_D is still the lowest.

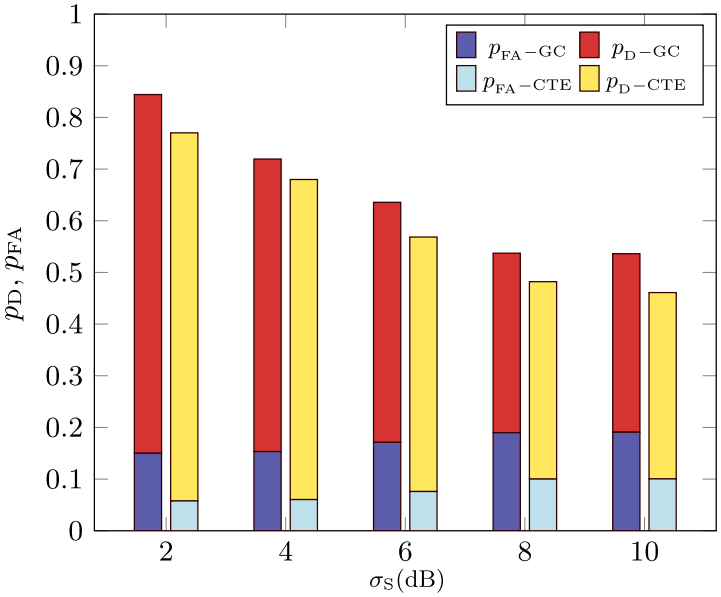

Fig. 4. p_{D} and p_{FA} of the topology sensing techniques varying the shadowing parameter $\sigma_{\mathrm{S}}(\mathrm{dB})$ for $\rho_{\mathrm{S}} = 0.3$ sensors/m^2.

6 Conclusion

This paper proposed a tool for non-collaborative wireless network topology inference using power profiles captured by radio-frequency (RF) sensors. The framework combines BSS, measurement association, excision filtering, and topology sensing. For the topology sensing, state-of-the-art techniques for causality inference such as Granger causality (GC) and conditional transfer entropy (CTE), that identify causal relationships between the separated traffic profiles, were adopted. The numerical results, accounting for realistic channel impairments (i.e., noise and shadowing) and packet collisions, showed that topology sensing is possible in this framework. As expected, the phenomena mentioned above degrade the performance of the BSS causing a non-perfect reconstruction of the power profile of the transmitted signals. Despite this, the proposed tool senses the topology with promising accuracy when operating in mild shadowing conditions, even with a relatively low number of RF sensors.

References

1. Al-Fuqaha, A., Guizani, M., Mohammadi, M., Aledhari, M., Ayyash, M.: Internet of things: a survey on enabling technologies, protocols, and applications. IEEE Commun. Surv. Tutor. **17**, 2347–2376 (2015)

2. Cichocki, A., et al.: Tensor decompositions for signal processing applications: from two-way to multiway component analysis. IEEE Signal Process. Mag. **32**(2), 145–163 (2015)
3. Cichocki, A., Zdunek, R., Amari, S.: New algorithms for non-negative matrix factorization in applications to blind source separation. In: IEEE International Conference on Acoustics Speech and Signal Processing Proceedings, vol. 5, Toulouse, France, June 2006
4. Favarelli, E., Testi, E., Pucci, L., Giorgetti, A.: Anomaly detection using WiFi signals of opportunity. In: IEEE International Conference on Signal Processing for Communication Systems (ICSPCS), Surfers Paradise, Gold Coast, Australia, December 2019
5. Granger, C.W.J.: Investigating causal relations by econometric models and cross-spectral methods. Econometrica **37**(3), 424–438 (1969)
6. Hyvarinen, A.: Fast and robust fixed-point algorithms for independent component analysis. IEEE Trans. Neural Netw. **10**(3), 626–634 (1999)
7. IEEE 802.22: Standard for Wireless Regional Area Networks-Part 22: Cognitive Wireless RAN Medium Access Control (MAC) and Physical Layer (PHY) specifications: Policies and procedures for operation in the TV Bands, July 2011
8. Ivkovic, G., Spasojevic, P., Seskar, I.: Localization of packet based radio transmitters in space, time, and frequency. In: Asilomar Conference on Signals, Systems and Computers. Pacific Grove, CA, USA, November 2008
9. Joho, M., Mathis, H., Lambert, R.H.: Overdetermined blind source separation: using more sensors than source signals in a noisy mixture. In: International Conference on Independent Component Analysis and Blind Signal Separation (ICA), Helsinki, Finland, pp. 81–86, June 2000
10. Kontos, T., Alyfantis, G.S., Angelopoulos, Y., Hadjiefthymiades, S.: A topology inference algorithm for wireless sensor networks. In: IEEE Symposium on Computers and Communications (ISCC), Cappadocia, Turkey, pp. 479–484, July 2012
11. Laghate, M., Cabric, D.: Learning wireless networks' topologies using asymmetric Granger causality. IEEE J. Sel. Topics Signal Process. **12**(1), 233–247 (2018). https://doi.org/10.1109/JSTSP.2017.2787478
12. Mariani, A., Giorgetti, A., Chiani, M.: Effects of noise power estimation on energy detection for cognitive radio applications. IEEE Trans. Commun. **59**(12), 3410–3420 (2011). https://doi.org/10.1109/TCOMM.2011.102011.100708
13. Mariani, A., Giorgetti, A., Chiani, M.: Model order selection based on information theoretic criteria: design of the penalty. IEEE Trans. Signal Process. **63**(11), 2779–2789 (2015)
14. Nurminen, H., Dashti, M., Piché, R.: A survey on wireless transmitter localization using signal strength measurements. Wirel. Commun. Mobile Comput. **2017**, 1–12 (2017)
15. Pahlavan, K., Li, X., Ylianttila, M., Chana, R., Latva-aho, M.: An overview of wireless indoor geolocation techniques and systems. In: Omidyar, C.G. (ed.) MWCN 2000. LNCS, vol. 1818, pp. 1–13. Springer, Heidelberg (2000). https://doi.org/10.1007/3-540-45494-2_1
16. Pearl, J.: Causality: Models, Reasoning and Inference, 2nd edn. Cambridge University Press, New York (2009)
17. Qin, X., Lee, W.: Statistical causality analysis of INFOSEC alert data. In: Vigna, G., Kruegel, C., Jonsson, E. (eds.) RAID 2003. LNCS, vol. 2820, pp. 73–93. Springer, Heidelberg (2003). https://doi.org/10.1007/978-3-540-45248-5_5
18. Schreiber, T.: Measuring information transfer. Phys. Rev. Lett. **85**, 461–464 (2000). https://doi.org/10.1103/PhysRevLett.85.461

19. Sharma, P., Bucci, D.J., Brahma, S.K., Varshney, P.K.: Communication network topology inference via transfer entropy. IEEE Trans. Netw. Sci. Eng. **7**, 1–7 (2019). https://doi.org/10.1109/TNSE.2018.2889454
20. Sithamparanathan, K., Giorgetti, A.: Cognitive Radio Techniques: Spectrum Sensing, Interference Mitigation and Localization. Artech House Publishers, Boston (2012)
21. Stoica, P., Selen, Y.: Model-order selection: a review of information criterion rules. IEEE Signal Proc. Mag. **21**(4), 36–47 (2004)
22. Testi, E., Favarelli, E., Giorgetti, A.: Machine learning for user traffic classification in wireless systems. In: European Signal Processing Conference (EUSIPCO), Rome, Italy, pp. 2040–2044, September 2018. https://doi.org/10.23919/EUSIPCO.2018.8553196
23. Testi, E., Favarelli, E., Pucci, L., Giorgetti, A.: Machine learning for wireless network topology inference. In: International Conference on Signal Processing and Communication Systems (ICSPCS), Surfers Paradise, Gold Coast, Australia, December 2019
24. Testi, E., Giorgetti, A.: Blind wireless network topology inference. IEEE Trans. Commun. **69**, 1109–1120 (2020)
25. Tilghman, P., Rosenbluth, D.: Inferring wireless communications links and network topology from externals using Granger causality. In: IEEE MILCOM, Military Communications Conference (MILCOM), San Diego, CA, USA, pp. 1284–1289, November 2013. https://doi.org/10.1109/MILCOM.2013.219
26. Urkowitz, H.: Energy detection of unknown deterministic signals. Proc. IEEE **55**(4), 523–531 (1967)
27. Wax, M., Kailath, T.: Detection of signals by information theoretic criteria. IEEE Trans. Acoust. Speech Signal Process **33**(2), 387–392 (1985)
28. Wenli, J., Teng, G., Meiyin, J.: Researching topology inference based on end-to-end date in wireless sensor networks. In: International Conference on Intelligent Computation Technology and Automation (ICICTA), Shenzhen, China, vol. 2, pp. 683–686, April 2011
29. Wibral, M., et al.: Measuring information-transfer delays. Plos One **8**, 1–19 (2013)
30. Xu, H., Farajtabar, M., Zha, H.: Learning Granger causality for Hawkes processes. In: International Conference on Machine Learning ICML, New York, NY, USA, vol. 48, February 2016
31. Yu, C., Chen, K., Cheng, S.: Cognitive radio network tomography. IEEE Trans. on Veh. Technol. **59**(4), 1980–1997 (2010)
32. Yu, X., Hu, D., Xu, J.: Blind Source Separation: Theory and Applications, 1st edn. Wiley, New York (2014)
33. Vardi, Y.: Network tomography: estimating source-destination traffic intensities from link data. J. Am. Stat. Assoc. **91**(433), 365–377 (1996)